









The mutational repertoire of uterine sarcomas and carcinosarcomas in a Brazilian cohort: A preliminary study

Leonardo Tomiatti da Costa ¹, Laura Gonzalez dos Anjos ¹, Luciane Tsukamoto Kagohara ^{1,II}, Giovana Tardin Torrezan ^{III}, Claudia A. Andrade De Paula ^{III}, Edmund Chada Baracat ^I, Dirce Maria Carraro ^{III}, Katia Candido Carvalho ^{I,*}

¹Laboratorio de Ginecologia Estrutural e Molecular, Disciplina de Ginecologia, Hospital das Clinicas (HCFMUSP), Faculdade de Medicina, Universidade de Sao Paulo, Sao Paulo, SP, BR. ^{II}School of Medicine, Sidney Kimmel Comprehensive Cancer Center, Johns Hopkins University, Baltimore, MD, USA. ^{III}Grupo de Biologia Molecular e Genomica, Centro A.C.Camargo, Sao Paulo, SP, BR.

da Costa LT, dos Anjos LG, Kagohara LT, Torrezan GT, De Paula CAA, Baracat EC, et al. The mutational repertoire of uterine sarcomas and carcinosarcomas in a Brazilian cohort: A preliminary study. *Clinics (Sao Paulo)*. 2021;76:e2324

*Corresponding author. E-mail: carvalhokc@gmail.com

OBJECTIVES: The present study aimed to contribute to the catalog of genetic mutations involved in the carcinogenic processes of uterine sarcomas (USs) and carcinosarcomas (UCSs), which may assist in the accurate diagnosis of, and selection of treatment regimens for, these conditions.

METHODS: We performed gene-targeted next-generation sequencing (NGS) of 409 cancer-related genes in 15 US (7 uterine leiomyosarcoma [ULMS], 7 endometrial stromal sarcoma [ESS], 1 adenosarcoma [ADS]), 5 UCS, and 3 uterine leiomyoma (ULM) samples. Quality, frequency, and functional filters were applied to select putative somatic variants.

RESULTS: Among the 23 samples evaluated in this study, 42 loss-of-function (LOF) mutations and 111 missense mutations were detected, with a total of 153 mutations. Among them, 66 mutations were observed in the Catalogue of Somatic Mutations in Cancer (COSMIC) database. *TP53* (48%), *ATM* (22%), and *PIK3CA* (17%) were the most frequently mutated genes. With respect to specific tumor subtypes, ESS showed mutations in the *PDE4DIP*, *IGTA10*, and *DST* genes, UCS exhibited mutations in *ERBB4*, and ULMS showed exclusive alterations in *NOTCH2* and *HER2*. Mutations in the *KMT2A* gene were observed exclusively in ULM and ULMS. *In silico* pathway analyses demonstrated that many genes mutated in ULMS and ESS have functions associated with the cellular response to hypoxia and cellular response to peptide hormone stimulus. In UCS and ADS, genes with most alterations have functions associated with phosphatidylinositol kinase activity and glycerophospholipid metabolic process.

CONCLUSION: This preliminary study observed pathogenic mutations in US and UCS samples. Further studies with a larger cohort and functional analyses will foster the development of a precision medicine-based approach for the treatment of US and UCS.

KEYWORDS: Sarcoma; Carcinosarcoma; Mutation; DNA Sequence Analysis.

INTRODUCTION

Sarcomas are rare heterogeneous tumors that affect the female genital tract and originate from tissues such as muscle, fat, bones, and fibrous tissue. Uterine sarcomas (USs) are the most commonly occurring gynecological sarcomas, representing 90% of the total cases (1). Based on their histological composition, uterine tumors with mesenchymal elements can

be divided into 1) pure sarcomas (uterine leiomyosarcomas - ULMSs, endometrial stromal sarcomas - ESSs); 2) mixed epithelial and mesenchymal tumors (adenosarcomas - ADSs), and 3) carcinosarcomas - UCSs, a biphasic tumor composed of high-grade carcinomatous and sarcomatous components derived from transdifferentiation of carcinoma (2). Many studies have characterized UCS tumors as mixed USs; however, since 2014, they have been reclassified as endometrial carcinomas (ECs) that demonstrate metaplastic features (3,4). Despite their low prevalence, USs are associated with high rates of local recurrence, distant metastases, and poor prognosis, with two-year survival rates below 50% (1).

Several genetic alterations have been associated with USs and UCSs, with few alterations being associated with specific histological subtypes. For instance, ESSs can be divided into two types: low-grade ESS (LG-ESS) and high-grade ESS (HG-ESS), both characterized by recurrent chromosomal translocations. In LG-ESS, the most common translocation,

Copyright © 2021 CLINICS – This is an Open Access article distributed under the terms of the Creative Commons License (<http://creativecommons.org/licenses/by/4.0/>) which permits unrestricted use, distribution, and reproduction in any medium or format, provided the original work is properly cited.

No potential conflict of interest was reported.

Received for publication on August 11, 2020. **Accepted for publication on** October 15, 2020

DOI: 10.6061/clinics/2021/e2324



t [7; 17] (p15; q21), is observed in almost 50% of the cases and results in the *JAZF1-SUZ12* gene fusion (5). Ma et al. (6), revealed that the JAZF1-SUZ12 fusion protein destabilizes polycomb repressive complex 2 (PRC2), abolishes histone methyltransferase (HMT) activity, and subsequently activates genes normally repressed by PRC2. JAZF1-PHF1, EPC1-PHF1, PHF1-MEAF6, MBTD1-CXorf67, and JAZF1-BCORL1 are other less frequent fusion proteins observed in the patients with these tumors. HG-ESS exhibits a *YWHAE-NUTM2* gene rearrangement (previously termed *YWHAE-FAM22*). Recently, molecular alterations in *ZC3H7B-BCOR*, *BCOR-ITD*, *EPC1-BCOR*, *JAZF1-BCORL1*, and *BRD8-PHF1* have been identified. This histological subtype demonstrates more aggressive clinical behavior and worse prognosis (5,2). Many previous studies have investigated the ESS genome with a focus on genetic fusions (7-10). However, Choi et al. (11) demonstrated that fusions are not the only genetic alterations that occur during the development of ESS. Using whole-exome sequencing methods, the aforementioned study described mutations in *PTEN*, *RB1*, *TP53*, and *CDH1*. Despite the use of a very small number of ESS samples in this study (3 LG-ESS), it is a valuable contribution to the understanding of the pathogenesis of such tumors.

ULMSs are not characterized by specific chromosome translocations; however, they are associated with a complex karyotype with chromosomal gains and losses, such as deletion in chromosome 1. Most ULMSs express *PDGFR- α* , *WT1*, *CYP19*, and *GNRH-R* (12,13). Owing to gene alterations, the loss of function in the tumor suppressor genes, *BRCA1* and *MED12* as well as the loss of expression of the proteasome β 1i subunit *LMP2* have been associated with ULMS development (14). Additionally, The Cancer Genome Atlas (TCGA) Research Network (15) examined the molecular characterization of adult soft tissue sarcomas (STSs) and observed that ULMSs shared more similarities with extrauterine LMSs than that with other sarcomas. Although both tumors exhibit the same pattern of cell differentiation, their tumor environments are extremely diverse. This study included 53 cases of soft-tissue LMS (extrauterine) and 27 ULMS cases that were evaluated by whole-exome sequencing, demonstrating frequent alterations in *TP53*, *RB1*, *ATRX*, and *MED12* (16).

Somatic mutations have also been described occurring at low frequency in the majority of the tyrosine kinase growth factor gene family and their targets, namely, v-raf murine sarcoma viral oncogene homolog B1 (*BRAF*), *CDKN2A*, epidermal growth factor receptor (*EGFR*), *HER2*, v-kit Hardy-Zuckerman 4 feline sarcoma viral oncogene homolog (*KIT*), v-Ki-ras2 Kirsten rat sarcoma viral oncogene homolog (*KRAS*), platelet-derived growth factor receptor (*PDGFR*), and phosphatidylinositol-4,5-bisphosphate 3-kinase, catalytic subunit α (*PI3KCA*) during the development of UCS. In addition, mutations in *TP53*, *PTEN*, protein phosphatase 2 scaffold subunit alpha (*PPP2R1A*), F-box, and WD repeat domain containing 7 (*FBXW7*) have already been identified, which may contribute to the development of therapeutic alternatives including the use of the inhibitors of PARP, *EZH2*, cell-cycle, and *PI3K* pathway (14,17). Little information is available on how mutations contribute to ADS etiology; however, one study observed that *DICER1* mutations are associated with the tumorigenic process in a small subset of such tumors (18).

Since these are rare tumors, only a few studies focusing on the definition of the mutational repertoire of the different

histological types of rare sarcomas have been conducted thus far. Therefore, studies focusing on the mutational characterization of these tumors are of paramount importance and will contribute to the discovery of new biomarkers for precision medicine-based approaches in the treatment of such neoplasms. Herein, we investigated the mutational profile of the samples obtained from patients with ULMSs, UCSs, ESSs, and ADSs, using a commercial panel containing 409 cancer-associated genes involved in apoptosis, signaling, transcription regulation, inflammation response, and growth factors-associated pathway.

■ MATERIALS AND METHODS

Sample selection

In order to analyze differences in genetic mutations between different histological types of US, we initially selected 43 formalin-fixed and paraffin-embedded (FFPE) human samples including 14 ULMS, 12 ESS, 2 ADS, 12 UCS, and 3 ULM–non-cancerous tumor (as reference samples). All samples were obtained via surgical procedures performed between 2000 and 2012 at the Institute of Cancer of Sao Paulo (ICESP) and Clinics Hospital of the Faculty of Medicine, University of Sao Paulo (HCFMUSP). Tissues were stored at the molecular and structural gynecology laboratory (LIM-58) of the University of Sao Paulo Medical School (FMUSP).

This study was performed in accordance with the Declaration of Helsinki and was approved by the Research Ethics Committee of the FMUSP with protocol number 477/15. Patients' medical records were revised and the following data were recorded: age at diagnosis, postmenopausal bleeding, adjuvant treatment, presence of metastasis or recurrence, and status.

DNA Isolation

Genomic DNA was extracted using the QIAamp DNA FFPE Tissue Kit obtained from QIAGEN[®] according to the manufacturer's instructions. DNA concentration, purity, and integrity were assessed by spectrophotometry (Nanodrop 2000, Thermo Fisher Scientific) and fluorometry (Qubit - Thermo Fisher Scientific), respectively.

Preparation of sequencing libraries and Next-Generation Sequencing (NGS)

Sequencing libraries were prepared using the Ion Torrent Ampliseq Comprehensive Cancer Panel - Catalog number: 4477685 (Thermo Fisher Scientific), which contains ~16,000 primer pairs multiplexed into 4 pools. This commercial panel was designed to assess the mutational profile of 409 cancer driver genes and drug targets along with signaling cascades, apoptosis genes, DNA repair genes, transcription regulators, inflammatory response genes, and growth factor genes (Table S1). Prior to amplification, DNA was treated with the uracil-DNA glycosylase enzyme (Thermo Fisher Scientific) by adding 1 unit of enzyme per 50 ng of DNA and incubating for 15 min at 37 °C. This procedure was performed to remove DNA molecules containing uracil and decrease the number of artifactual variants in the sequencing (19). Libraries were then prepared using Ion AmpliSeq[™] Library kit 2.0 protocols, with 10 ng of input DNA per pool, totaling 40 ng of DNA from each sample. The FuPa reagent was used to partially digest primer sequences and phosphorylate the amplicons. Next, sequencing adaptors and barcodes were ligated to the amplicon by the enzyme Ligase using the Ion



Xpress™ Barcode Adapters kit (Thermo Fisher Scientific), which were then purified using magnetic beads (Agen-court® AMPure® XP Reagents, Beckman Coulter). Subsequently, emulsion PCR was performed using the Ion PI™ Hi-Q™ OT2 200 Kit (Thermo Fisher Scientific), followed by sequencing with Ion PI™ Hi-Q™ sequencing 200 and Ion PI™ Chip.

Data Analysis

The results were analyzed using the Torrent Suite v5.0.5 software (Thermo Fisher Scientific). Sequence variants (SNVs and indels) were identified using the Torrent Variant Caller (Ion Torrent – Thermo Fisher Scientific) and compared to the GRCh37 / hg19 genome version. VCF files were analyzed using VarSeq v1.8 software (GoldenHelix) for variant annotation and prioritization. The variants were filtered based on the quality and frequency criteria: coverage (>100), genotype quality score cutoff (GQS>50), variant base in at least 5% of reads, variant base present in at least 2 reads in each direction, homopolymer-length error<5, absence of genetic variants in population databases (ExAC; NHLBI-ESP; 1000 Genomes Project) or minor allele frequency (MAF)≤0.01%.

Subsequently, variants were selected based on their effect on protein expression, with the following being considered: 1) variants described in the COSMIC database; 2) loss-of-function variants – Frameshift variants–nucleotide insertions/deletions, gain/loss of stop codons, splice site alterations; or 3) missense variants (in-frame insertions/deletions, amino acid exchange) predicted as possibly pathogenic in at least three of six prediction programs used (SIFT, PolyPhen, MutationTaster, MutationAssessor, FATHMM, FATHMM-MKL) and occurring in oncogenes or tumor suppressor genes in OncoMD database. Variants not previously described in the COSMIC database were visually inspected using the integrative genomics viewer (IGV) program to exclude sequencing artifacts.

Construction of genetic interaction networks was performed using Cytoscape platform version 3.7.0, which uses data from protein and genetic interactions, pathways, co-expression, co-localization, and protein domain similarity.

RESULTS

Initially, 40 US and UCS (14 ULMS, 12 ESS, 2 ADS, and 12 UCS) and 3 ULM samples were selected from the pathology department files; however, only 23 (7 ULMS, 7 ESS, 1 ADS, 5 UCS, and 3 ULM) remained until the end of NGS analyses. Some losses occurred while performing multiplex PCR reactions (AmpliSeq™), during which we observed a high degree of fragmented DNA and many genetic artifacts in several samples. These issues are expected since tissue processing for paraffin inclusion and long storage time causes damage to the DNA structure (integrity). The clinical and pathological features of 40 patients with US and UCS who were enrolled in this study are summarized in Table 1.

Among the 23 samples deemed suitable for the evaluation of sequencing data, homogeneity average was 73.2%, median base coverage was 1257X, and horizontal coverage was 84.3% corresponding to 100X. Based on the NGS data, we selected point mutations with possible impacts on the function of the protein encoded by the altered gene (missense, nonsense, splice-site mutations, loss of stop codons) and small insertions and deletions (indels). Total variants detected in each sample and filtered variants for the

Table 1 - Clinical and pathological features of US and UCS patients (n=40).

Variables	Categories	US/UCS n (%)
Age	> 50 years	33 (82)
	≤50 years	7 (18)
	N.A.	0 (0)
Postmenopausal Bleeding	Yes	22 (55)
	No	13 (33)
	N.A.	5 (12)
Adjuvant Treatment	No	8 (20)
	RT	19 (47)
	CT	8 (20)
	RT + CT	5 (13)
	N.A.	0 (0)
Metastasis or Recurrence	Yes	22 (55)
	No	14 (35)
	N.A.	4 (10)
Status	Alive	11 (27)
	Death	23 (58)
	Loss of follow-up	6 (15)
	N.A.	0 (0)

radiotherapy (RT); chemotherapy (CT); not available (NA); uterine sarcomas (US).

*ULM samples were not included owing to their benign characterization.

selection of somatic alterations of interest are presented in Table 2.

An average of 1700 alterations were identified per sample (ranging from 746 to 3521), with an average of 1606 single nucleotide variants (SNVs) (ranging from 678 to 3406), 40 insertions (ranging from 23 to 77), and 55 deletions (ranging from 25 to 114). To select relevant somatic variants, a first filter was applied focusing on the quality and frequencies of these alterations. A second filter, focusing on variant functions and effects, was used to select the alterations that would be most relevant in alterations of gene functions. Collectively, in 23 samples that were evaluated, 42 LOF mutations and 111 missense mutations were detected, with a total of 153 filtered mutations, among which 66 were found in the COSMIC database (Table 2).

Among the 409 genes included in the panel, mutations were detected in 94 distinct genes, with 30 genes demonstrating mutations in more than one sample and 64 genes showing mutations in a single sample. Table 3 presents the list of genes that were mutated in more than one sample of the cohort, along with the number of mutated samples and the histological types. *TP53* (11/23 – 48%), *ATM* (5/23 – 22%), and *PIK3CA* (4/23 – 17%) were the most frequently mutated genes.

The Venn diagram (Figure 1) shows the shared and individual (specific) mutations of each malignant histological subtype evaluated (ULMS, ESS, UCS, and ADS). Three shared genes were observed (*ATM*, *TP53*, and *KMT2D*) among the ULMS, ESS, and UCS samples. Nineteen genes were shared between 2 types of tumors, and 68 genes were mutated in a single type. Among them, 6 genes were mutated in more than one sample of the same histological subtype, namely, *PDE4DIP* (3 ESS samples), *ITGA10*, and *DST* (2 ESS samples), *NOTCH2*, and *HER2* (2 ULMS samples), and *ERBB4* (2 UCS samples). Quantitatively, this analysis shows similarities in the mutational profiles of ULMS and ESS, with 6 mutated genes in common (6.7%) between both subtypes. In the genes *JAK3*, *APC*, *ATRX*, *CREBBP*, *MYB*, and *SYNE1*, most of the mutations were characterized as missense mutations; however, in the *SYNE1* gene, the two mutations



Table 2 - Total variants obtained after filtering performed to increase the specificity of NGS results (higher stringency).

Samples	General (pre-filters)				Selected Variants		
	Total	SNV	Insertions	Deletions	LOFs	Missense	Cosmic
ESS 2	2347	2257	40	50	1	6	5
ESS 3	1551	1473	31	47	2	6	4
ESS 4	1249	1162	36	51	1	1	1
ESS 5	1416	1324	36	56	0	4	3
ESS 7	1494	1397	40	57	2	2	1
ESS 9	1421	1343	35	43	1	6	5
ESS 10	1440	1329	35	76	4	6	6
UCS 2	1332	1223	47	62	3	4	4
UCS 5	1362	1271	42	49	7	13	7
UCS 9	1972	1884	42	46	1	6	4
UCS 13	1234	1150	36	48	1	6	4
UCS 19	1604	1516	33	55	1	3	3
ULMS 38	746	678	43	25	0	7	4
ULMS 39	1768	1688	34	46	1	2	2
ULMS 40	1296	1193	42	61	2	3	1
ULMS 45	2004	1921	36	47	2	3	1
ULMS 52	2806	2746	23	37	0	11	6
ULMS 50	2842	2651	77	114	0	1	0
ULMS 59	2132	1968	76	88	4	6	2
ADS 2	3521	3406	41	74	6	10	0
ULM 119	1298	1201	37	60	1	1	0
ULM 143	981	919	33	29	1	2	2
ULM 152	1297	1237	25	35	1	2	1

*Endometrial stromal sarcoma (ESS); Uterine carcinosarcoma (UCS); Uterine leiomyosarcoma (ULMS); Adenocarcinoma (ADS); Uterine leiomyoma (ULM). Single nucleotide variant (SNV); Loss of function (LOFs); Catalogue of Somatic Mutations in Cancer (COSMIC).

Table 3 - Gene mutations observed in more than one sample and histological subtypes.

Gene	Mutated samples n (%)	Histological Types (ULMS/ESS/UCS/ADS/ULM)
TP53	11 (48%)	4 ULMS, 3 ESS, 4 UCS
ATM	5 (22%)	2 ULMS, 2 ESS, 1 UCS
PIK3CA	4 (17%)	1 ESS, 3 UCS
KMT2D	3 (13%)	1 ULMS, 1 ESS, 1 UCS
MTOR	3 (13%)	1 ESS, 1 UCS, 1 ULM
JAK3	3 (13%)	1 ULMS, 1 ESS, 1 ULM
APC	3 (13%)	1 ULMS, 2 ESS
DICER1	3 (13%)	1 ESS, 2 UCS
TRRAP	3 (13%)	2 UCS, 1 ADS
TSC2	3 (13%)	2 ULMS, 1 ADS
PDE4DIP	3 (13%)	3 ESS
AR	2 (9%)	1 ESS, 1 UCS
ATRX	2 (9%)	1 ULMS, 1 ESS
CREBBP	2 (9%)	1 ULMS, 1 ESS
DNMT3A	2 (9%)	1 UCS, 1 ADS
EPHA7	2 (9%)	1 UCS, 1 ADS
KAT6B	2 (9%)	1 UCS, 1 ADS
KMT2A	2 (9%)	1 ULMS, 1 ULM
MET	2 (9%)	1 UCS, 1 ULM
MYB	2 (9%)	1 ULMS, 1 ESS
NOTCH1	2 (9%)	1 ULMS, 1 UCS
PRKDC	2 (9%)	1 UCS, 1 ADS
SYNE1	2 (9%)	1 ULMS, 1 ESS
NF1	2 (9%)	1 ESS, 1 UCS
NOTCH2	2 (9%)	2 ULMS
HER2	2 (9%)	2 ULMS
ERBB4	2 (9%)	2 UCS
DAXX	2 (9%)	1 ESS, 1 ADS
ITGA10	2 (9%)	2 ESS
DST	2 (9%)	2 ESS

observed in ULMS and ESS samples were determined as LOF mutations (c.352C>T and c.8565G>A, respectively). In addition, mutations in the TRRAP, DNMT3A, EPHA7, KAT6B, and

PRKDC genes indicate that UCS and ADS may exhibit molecular similarities.

Table 4 summarizes the genes with the most frequent alterations (mutations in 2 or more samples, or with 2 mutations in the same sample), the types of mutations, and their position. Alterations in the respective proteins are also indicated, along with the combined effect of these alterations (Missense or LOF) and DNA (c.), and protein (p.) nomenclatures. Their nomenclature can be used for database searches. The descriptions of the 153 potentially somatic variants are listed in Table S2. UCS5, ULMS52, ESS58107, and ADS2 samples demonstrated the highest number of mutations (UCS5 with 20 mutations in 19 genes; ULMS52 with 11 mutations in 10 genes; ESS58107 with 10 mutations in 10 genes, and ADS2 with 16 mutations in 16 genes). Samples with the lowest number of mutations were ULMS50b with 1 mutation in ALK, ESS4 with 2 mutations (ATM and CREBBP), and ULM119 (benign tissue) with 2 mutations (MET and PDGFB).

Based on the data described in Table 4, we selected genes with more than three mutations in our cohort to submit to the OncoPrinter visualization tool (cBioPortal - <http://www.cbioportal.org/>). Figure 2 shows the percentage of patients demonstrating mutations in each gene, distribution, and the types of mutations observed in each sample. The highest frequency of gene mutations was observed in TP53 (48%) with the highest frequency of missense-type mutations (3 ULMS, 1 ESS, and 4 UCS samples). ATM mutations were observed in 22% of the samples, with 3 missense-type mutations (2 ULMS and 1 ESS) and 2 LOF-type mutations (1 ESS and 1 UCS). PIK3CA appeared to be the third most mutated gene (17%) present in 3 UCS samples, with most of the mutations determined as the missense-type. APC, MTOR, DICER1, TRRAP, KMT2D, TSC2, PDE4DIP, and JAK3 showed a 13% mutational frequency. LOF mutations in PDE4DIP was found exclusively/specifically in the ESS

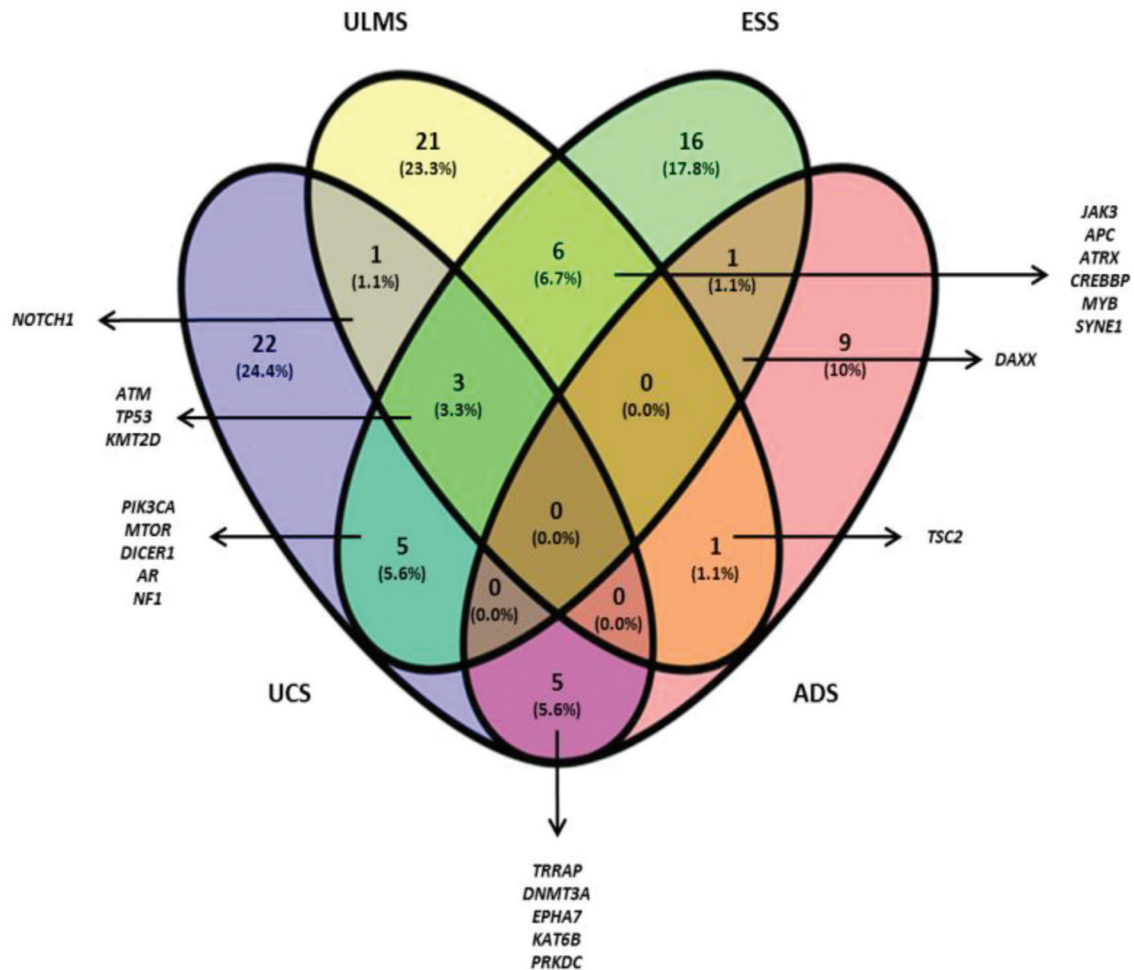


Figure 1 - Venn diagram (Oliveros J.C, 2015) constructed using the genetic sequencing data obtained from all samples. The numbers represent shared and individual mutations for each assessed histological type.

samples. *NF1*, *CREBBP*, and *MYB* demonstrated a 9% mutational frequency. Missense mutations in *CREBBP* and *MYB* were associated with ULMS and ESS (4 mutations in ULMS and 2 in ESS).

Since uterine sarcomas are histologically classified into two primary subtypes, we used the same classification to study the association of the mutated genes with pure sarcomas (ULMS – ESS) and mixed tumors (UCS – ADS). Figure 3 shows the association of the mutated genes in the group of tumors classified as pure (ULMS and ESS). According to the Cytoscape platform (20), many genes demonstrating mutations in these histological subtypes exhibit functions associated with the cellular response to hypoxia (*MTOR*, *PDK1*, *MDM2*, *TP53*, *CREBBP*, *NOTCH1*, and *HIF1A*) and peptide hormone stimulus (*EIF4EBP1*, *RPTOR*, *TSC2*, *TSC1*, *MTOR*, *JAK3*, *ADCY6*, *PIK3CA*, *GNAS*, and *ATP6V1D*).

Although UCS is no longer classified as uterine sarcoma but as metaplastic carcinoma, we included this tumor group in the analysis shown in Figure 4. Here, we associated UCS – ADS owing to their mixed histologies (epithelial and mesenchymal components) and also because many retrospective studies on the US still include UCS in their available samples. According to the Cytoscape platform (20), many mutated genes in these tumors have functions associated with phosphatidylinositol kinase activity (*PI4K2A*, *PIK3CA*,

PIK3CB, *ATM*, *PI4KB*, *PIK3CG*, *PIK3C2B*, *PI4KA*, *PIK3C2A*, *PIK3C3*, *PIK3C2G*, and *PIK3CD*) and glycerophospholipid metabolic process (*PI4K2A*, *PIK3CA*, *PIK3CB*, *ATM*, *PI4KB*, *PIK3CG*, *PIK3C2B*, *PI4KA*, *PIK3C2A*, *PIK3C3*, *PIK3C2G*, *PIK3CD*, *PI4K2B*, and *SMG1*).

Collectively, our results indicate that despite the molecular heterogeneity demonstrated by USs and UCSs, they share similarities in their mutational profiles. In addition, genetic interaction networks indicate that alterations in functions associated with hypoxia, response to peptide hormone stimulus in ULMSs and ESSs, and phosphatidylinositol kinase activity and glycerophospholipid metabolic process in UCS and ADS can influence the carcinogenic process of these tumors. Considering that NGS technology can provide a reliable molecular portrait of neoplasms quickly and cost-effectively (21), these results open new avenues for research and consequently, may positively impact the clinical management of patients with such tumors.

DISCUSSION

In this study, we performed a mutational screening of the samples collected from patients with USs and UCSs. We employed a panel of 409 genes for the screening. Initially, we focused on the mutated genes shared among more than



Table 4 - Most common mutations observed in the study, their chromosomal positions, effects, and nomenclature.

Sample	Chr:Pos	Gene	HGVS c.	HGVS p.	Effect
UCS2	3:178921549	<i>PIK3CA</i>	c.1031T>C	p.Val344Ala	Missense
	6:94120318	<i>EPHA7</i>	c.733G>A	p.Ala245Thr	Missense
	7:116339356	<i>MET</i>	c.218T>A	p.Leu73Ter	LOF: stop - gained
	8:48776121	<i>PRKDC</i>	c.5586delT	p.Phe1862Leufs	LOF: frameshift
UCS5	17:7577547	<i>TP53</i>	c.734G>T	p.Gly245Val	Missense
	1:11227575	<i>MTOR</i>	c.4254-1G>A	r.spl?	LOF: splice - acceptor
	3:178952085	<i>PIK3CA</i>	c.3140A>G	p.His1047Arg	Missense
	10:76735809	<i>KAT6B</i>	c.1714C>T	p.Arg572Cys	Missense
	11:108114777	<i>ATM</i>	c.594C>A	p.Cys198Ter	LOF: stop - gained
	14:95572101	<i>DICER1</i>	c.3007C>T	p.Arg1003Ter	LOF: stop - gained
	17:29588751	<i>NF1</i>	c.4600C>T	p.Arg1534Ter	LOF: stop - gained
	17:29665110	<i>NF1</i>	c.6772C>T	p.Arg2258Ter	LOF: stop - gained
	2:25469168	<i>DNMT3A</i>	c.1290T>G	p.Asn430Lys	Missense
	2:212587219	<i>ERBB4</i>	c.782A>C	p.Gln261Pro	Missense
	7:98513427	<i>TRRAP</i>	c.2281C>T	p.Arg761Trp	Missense
	X:66766207	<i>AR</i>	c.1219C>T	p.Arg407Cys	Missense
	UCS9	9:139391355	<i>NOTCH1</i>	c.6836C>T	p.Ala2279Val
12:49444719		<i>KMT2D</i>	c.2747C>T	p.Pro916Leu	Missense
17:7578442		<i>TP53</i>	c.488A>G	p.Tyr163Cys	Missense
UCS13	3:178916854	<i>PIK3CA</i>	c.241G>A	p.Glu81Lys	Missense
	14:95574253	<i>DICER1</i>	c.2614G>A	p.Ala872Thr	Missense
	17:7577534	<i>TP53</i>	c.747G>T	p.Arg249Ser	Missense
UCS19	7:98609947	<i>TRRAP</i>	c.11549G>A	p.Arg3850His	Missense
	2:212295800	<i>ERBB4</i>	c.2513G>A	p.Arg838Gln	Missense
ULMS38	17:7577580	<i>TP53</i>	c.701A>G	p.Tyr234Cys	Missense
	1:120458122	<i>NOTCH2</i>	c.7223T>A	p.Leu2408His	Missense
ULMS39	17:37864584	<i>HER2</i>	c.236A>C	p.Glu79Ala	Missense
	19:17937659	<i>JAK3</i>	c.3268G>A	p.Ala1090Thr	Missense
ULMS40	17:7577545	<i>TP53</i>	c.736A>G	p.Met246Val	Missense
	11:108139268	<i>ATM</i>	c.2770C>T	p.Arg924Trp	Missense
ULMS45	17:7577120	<i>TP53</i>	c.818G>A	p.Arg273His	Missense
	17:37881117	<i>HER2</i>	c.2446C>T	p.Arg816Cys	Missense
	X:76891445	<i>ATRX</i>	c.4660A>T	p.Arg1554Ter	LOF: stop - gained
	11:108160506	<i>ATM</i>	c.4414T>G	p.Leu1472Val	Missense
ULMS52	17:7578290	<i>TP53</i>	c.560-1G>C	r.spl?	LOF: splice - acceptor
	16:2135281	<i>TSC2</i>	c.4620C>A	p.Tyr1540Ter	LOF: stop - gained
	1:120459251	<i>NOTCH2</i>	c.6094C>A	p.His2032Asn	Missense
	9:139400980	<i>NOTCH1</i>	c.4013C>T	p.Ala1338Val	Missense
	11:118377142	<i>KMT2A</i>	c.10535C>T	p.Pro3512Leu	Missense
	12:49416396	<i>KMT2D</i>	c.16315C>T	p.Arg5439Trp	Missense
	16:2130319	<i>TSC2</i>	c.3551C>T	p.Ala1184Val	Missense
	16:3779521	<i>CREBBP</i>	c.5527T>C	p.Cys1843Arg	Missense
	16:3790470	<i>CREBBP</i>	c.4063G>A	p.Gly1355Arg	Missense
	17:7574017	<i>TP53</i>	c.1010G>A	p.Arg337His	Missense
ULMS59	5:112173857	<i>APC</i>	c.2566C>T	p.Arg856Cys	Missense
	6:135511289	<i>MYB</i>	c.331G>A	p.Gly111Ser	Missense
ULMS59	6:135539101	<i>MYB</i>	c.2269C>T	p.Arg757Trp	Missense
	6:152832196	<i>SYNE1</i>	c.352C>T	p.Arg118Ter	LOF: stop - gained
ULMS59	20:57429026	<i>GNAS</i>	c.706G>A	p.Asp236Asn	Missense
	20:57480457	<i>GNAS</i>	c.2381A>C	p.Lys794Thr	Missense
ESS2 (LG-ESS)	6:152706896	<i>SYNE1</i>	c.8565G>A	p.Trp2855Ter	LOF: stop - gained
	11:108175463	<i>ATM</i>	c.5558A>T	p.Asp1853Val	Missense
	17:7577121	<i>TP53</i>	c.817C>T	p.Arg273Cys	Missense
ESS2	17:7577139	<i>TP53</i>	c.799C>T	p.Arg267Trp	Missense
ESS3	1:145015874	<i>PDE4DIP</i>	c.214C>T	p.Arg72Ter	LOF: stop - gained
	5:112154777	<i>APC</i>	c.1048T>C	p.Ser350Pro	Missense
	5:112162855	<i>APC</i>	c.1459G>A	p.Gly487Arg	Missense
	6:56328464	<i>DST</i>	c.16429C>T	p.Arg5477Trp	Missense
	12:49418436	<i>KMT2D</i>	c.15977T>C	p.Leu5326Pro	Missense
	17:7578176	<i>TP53</i>	c.672 + 1G>A	r.spl?	LOF: splice - donor
	17:29556250	<i>NF1</i>	c.2617C>T	p.Arg873Cys	Missense
	17:29677234	<i>NF1</i>	c.7355G>T	p.Arg2452Leu	Missense
ESS4	11:108141990	<i>ATM</i>	c.2934delT	p.Leu979Cysfs	LOF: frameshift
	16:3820773	<i>CREBBP</i>	c.2678C>T	p.Ser893Leu	Missense
ESS5	1:11217330	<i>MTOR</i>	c.4348T>G	p.Tyr1450Asp	Missense
	19:17937659	<i>JAK3</i>	c.3268G>A	p.Ala1090Thr	Missense
ESS7	6:33287248	<i>DAXX</i>	c.1885G>A	p.Val629Ile	Missense
	14:95590677	<i>DICER1</i>	c.1232C>A	p.Ser411Ter	LOF: stop - gained
ESS7	X:76939115	<i>ATRX</i>	c.1633C>G	p.Gln545Glu	Missense



Table 4 - Continued.

Sample	Chr:Pos	Gene	HGVSc	HGVSp	Effect
ESS9	1:144906139	<i>PDE4DIP</i>	c.2494delC	p.Gln832Argfs	LOF - frameshift
	1:145536012	<i>ITGA10</i>	c.2104G>A	p.Ala702Thr	Missense
	3:178936091	<i>PIK3CA</i>	c.1633G>A	p.Glu545Lys	Missense
	5:112175711	<i>APC</i>	c.4420G>A	p.Ala1474Thr	Missense
ESS58107	1:145015874	<i>PDE4DIP</i>	c.214C>T	p.Arg72Ter	LOF: stop - gained
	1:145536012	<i>ITGA10</i>	c.2104G>A	p.Ala702Thr	Missense
	6:56328464	<i>DST</i>	c.16429C>T	p.Arg5477Trp	Missense
	6:135516944	<i>MYB</i>	c.1007C>T	p.Thr336Ile	Missense
	17:7578176	<i>TP53</i>	c.672 + 1G>A	r.spl?	LOF: splice - donor
	X:66863156	<i>AR</i>	c.1675A>T	p.Thr559Ser	Missense
ADS2	2:25467477	<i>DNMT3A</i>	c.1599C>A	p.Tyr533Ter	LOF: stop - gained
	6:33288629	<i>DAXX</i>	c.959A>G	p.Gln320Arg	Missense
	6:93979315	<i>EPHA7</i>	c.1513C>A	p.Leu505Met	Missense
	7:98501128	<i>TRRAP</i>	c.1024G>T	p.Glu342Ter	LOF: stop - gained
	8:48711786	<i>PRKDC</i>	c.10279G>T	p.Glu3427Ter	LOF: stop - gained
	10:76781925	<i>KAT6B</i>	c.3308_3310delAAG	p.Glu1104del	LOF: inframe/del
ULM119	16:2138078	<i>TSC2</i>	c.5098G>T	p.Ala1700Ser	Missense
	7:116403114	<i>MET</i>	c.2429A>C	p.His810Pro	Missense
ULM143	1:11307996	<i>MTOR</i>	c.995_996dupGG	p.Leu333Glyfs	LOF: frameshift
ULM152	19:17945696	<i>JAK3</i>	c.2164G>A	p.Val722Ile	Missense
	11:118344893	<i>KMT2A</i>	c.3019G>T	p.Gly1007Cys	Missense

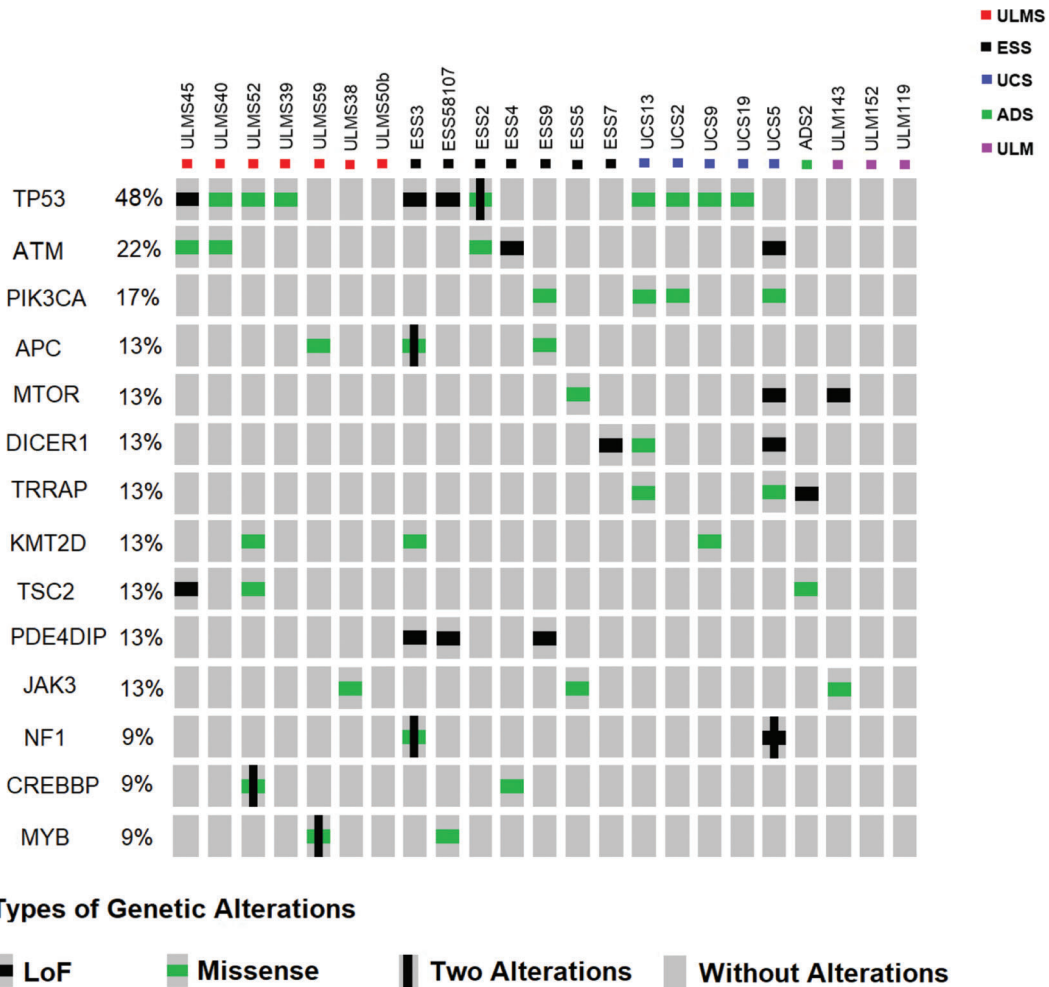


Figure 2 - Distribution of mutations in samples and their biological effects. The figure was constructed using the OncoPrinter from cBioPortal for Cancer Genomics database (<http://www.cbioportal.org/>). Each gray rectangle represents a sample according to the sequence indicated at the top. Genes with the highest frequency of alterations are shown. Captions for each type of alteration (Loss of function - Black Square; Missense - Green Square; Two alterations in the same gene - vertical line [modified by authors]; No alteration - gray rectangle) are indicated.

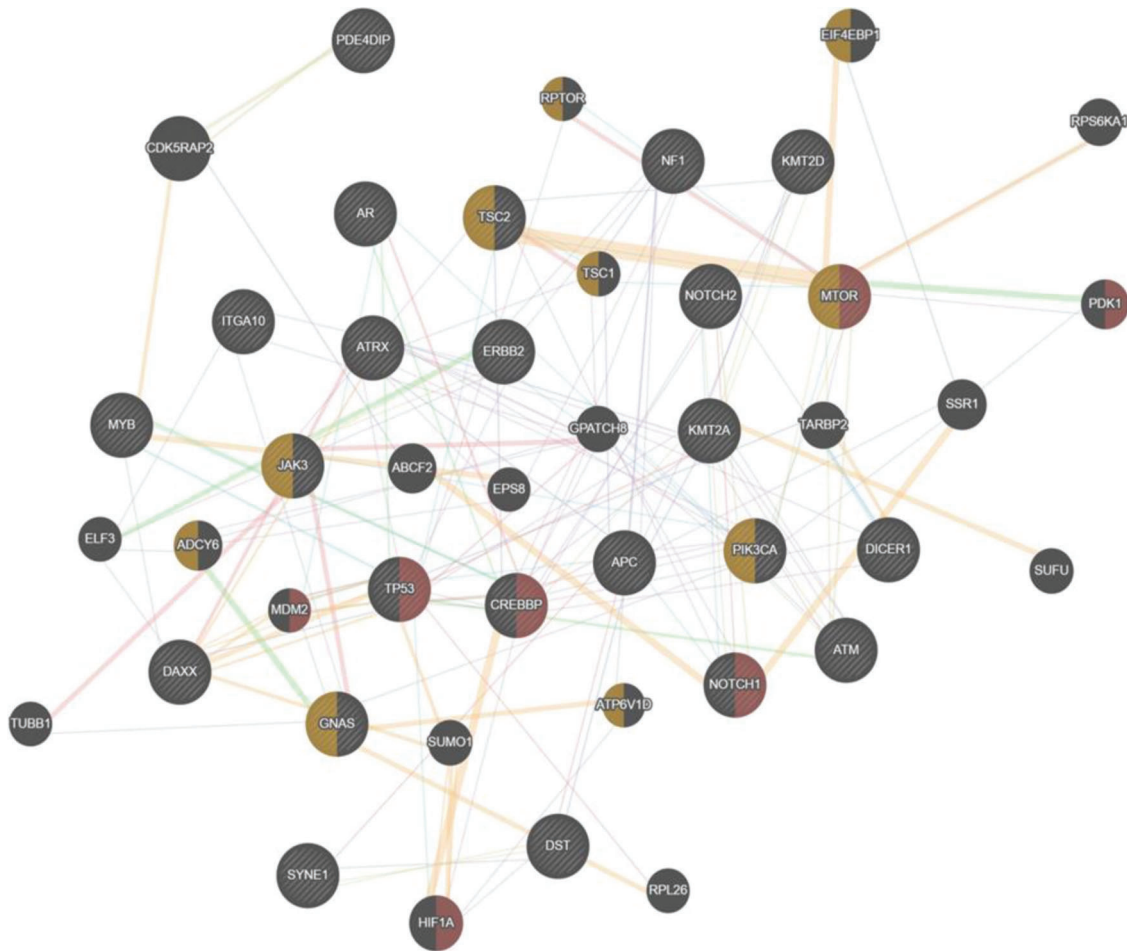


Figure 3 - Interaction network of mutated genes in the histological types of pure sarcomas (ULMS - ESS) prepared by the Cytoscape 3.7.0 platform. The network shows patterns of predicted interaction (orange); physical interactions (red); co-expression (violet); shared proteins domains (yellow); co-localization (blue), and genetic interaction (green). Red-labeled genes have a function associated with the cellular response to hypoxia and yellow-labeled genes have a function associated with the cellular response to the peptide hormone stimulus. The genes that were inserted to perform the analysis are shown with cross-hatched circles of a uniform size. The relevant genes are shown with solid circles whose size is proportional to the number of interactions. The reported link weights are indicated visually by line thickness.

one histological subtype of US. We initiated our analyses with 40 samples, but owing to the quality of the FFPE material, certain losses reduced the number of samples to 23. Considering the published reports on sarcomas, the number of samples was sufficient for this type of population mutational screening. In UCS and ESS samples, we identified mutations in genes that demonstrated alterations in previous studies conducted for examining other tumors, such as *PIK3CA*, *DICER1*, *AR*, and *NF1* (22). Although the role of these genes is known in different cancers, their role in the tumorigenesis of USs and USCs is not fully understood.

The *PIK3CA* gene encodes the p110 α protein, the catalytic subunit of PI3K, which controls the growth, division, survival, movement, and structure of cells. Many studies have demonstrated the importance of *PIK3CA* mutation in mediating tumorigenesis via increased *PI3K/AKT/mTOR* signaling (23,24). While investigating druggable molecular targets in uterine sarcomas, Cuppens et. al (25) identified *PI3K/MTOR* as a potential target in 26% of cases, which were primarily ULMS, HG-ESS, and undifferentiated uterine sarcomas. Here, we included eight samples of ESS. Seven of these

were characterized as HG-ESS, consistent with the molecular findings described in previous reports published for these tumors. *DICER1* is critical for the regulation of expression of several miRNAs. The *DICER1* gene is highly conserved among various species, indicating that mutations may compromise its function and might be involved in the onset of tumors (26). Previous reports published by our group (2,27) demonstrated the regulation of microRNAs associated with several oncogenic pathways, including *DICER1*. Mutations in *NF1* have already been demonstrated in soft-tissue sarcomas (myxofibrosarcomas and pleomorphic liposarcomas) (28). The expression of the androgen receptor (*AR*) seems to be associated with a better prognosis in patients with ESS. *AR* expression is higher in pre-malignant lesions and low-grade tumors (LG-ESS) (29). These findings may explain why *AR* expression is low in ULMS, which is an extremely aggressive tumor (30). However, the effects of the mutations observed in this gene need to be further investigated for US.

It is important to note that *NOTCH1* was the unique gene that shared mutations in the UCS and ULMS. Similarly,

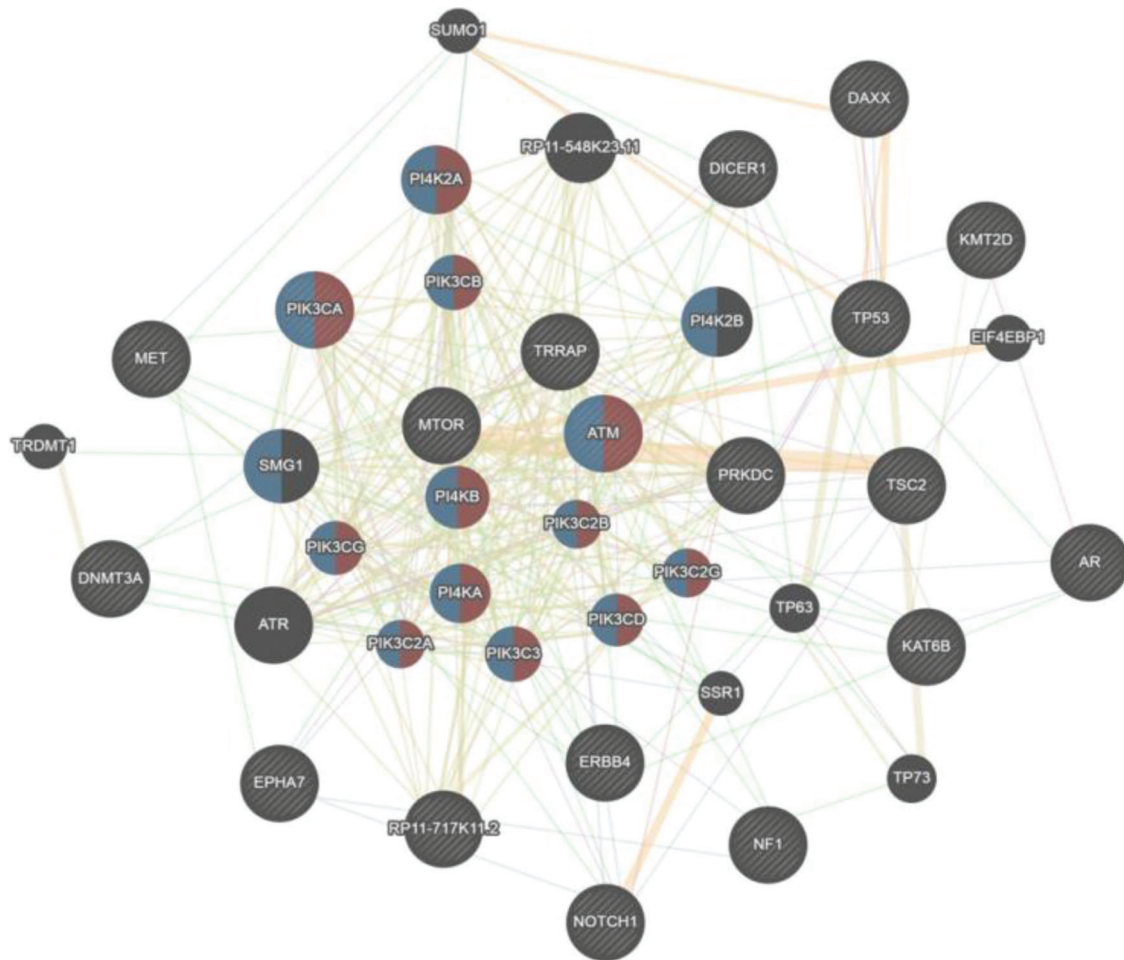


Figure 4 - Interaction network of mutated genes in mixed tumors (UCS - ADS) prepared by the Cytoscape 3.7.0 platform. The network shows patterns of predicted interaction (orange); physical interactions (red); co-expression (violet); shared proteins domains (yellow); co-localization (blue) and genetic interaction (green). Red-labeled genes have a function associated with phosphatidylinositol kinase activity and blue-labeled genes have a function associated with the glycerophospholipid metabolic process. The genes that were inserted to perform the analysis are shown with cross-hatched circles of a uniform size. The relevant genes are shown with solid circles whose size is proportional to the number of interactions. The reported link weights are indicated visually by line thickness.

mutations in the *DAXX* gene have also been observed in the cases of ESS/ADS and ULMS/ADS, which share mutations in *TSC2*. Thus, our results suggest that besides exhibiting a similar tumor microenvironment, USs and UCSs also share genetic alterations. This observation is relevant to the understanding of the onset and evolution of these tumors. Furthermore, ULMS cases originating from ULMs have been reported; however, this hypothesis has not been proven yet (31,32). Our study showed that mutations in *KMT2A* were exclusively observed in ULMS and ULM. The c.3019G>T variant appears to be related to the Wiedemann-Steiner syndrome and Kabuki syndrome (33,34).

We attempted to identify specific genes for each type of tumor, establishing individual signatures. Despite the heterogeneity, we were able to identify six specific genes for three of the histological types evaluated in this study. In ESS samples, we observed variants in the *PDE4DIP* (c.214C>T and c.2494delC), *ITGA10* (c.2104G>A), and *DST* (c.16429C>T) genes. The variant *PDE4DIP* c.214C>T is described in the COSMIC database (35) and was first observed in papillary thyroid carcinoma. Mutations in this gene are described in several tumors, such as breast cancer as well as

the cancers of the endometrium, cervix, ovaries, and urinary tract. The protein encoded by the *PDE4DIP* gene is responsible for binding 4D phosphodiesterase to the Golgi complex. Alterations in this gene may cause a myeloproliferative disorder associated with eosinophilia (36). Despite the information available in databases and the literature, its typical role in tumor biology remains unknown.

In UCS, we observed two variants of *ERBB4* (c.782A>C and c.2513G>A). The variant *ERBB4* c.2513G>A is described in the COSMIC database (35) as pathogenic (score 0.99) and has already been observed in hormone receptor-positive breast cancer, large bowel adenocarcinoma, malignant melanoma, and gastroesophageal junction adenocarcinoma. The role of *ERBB4* as a tumor progression factor is not fully elucidated. However, this gene is known to be overexpressed and/or mutated in several solid tumors (37). The monoclonal antibody *ERBB4* therapy is effective in breast, lung, and prostate cancer cells *in vitro* and *in vivo* (38). Specific and detailed studies may demonstrate new opportunities for the development of therapies targeting these tumors.

Mutations in *NOTCH2* and *HER2* have also been observed exclusively in ULMS. All variants are described in the



COSMIC database (35). c.6094C>A mutation of *NOTCH2* is considered to be pathogenic (score 0.97) and is described in diffuse large B cell lymphoma and pancreatic ductal adenocarcinoma (PDAC). The *NOTCH2* c.7223T>A variant is also pathogenic (score 0.85) and has already been described in meningioma, a primary non-malignant CNS tumor (39). *HER2* also presented two pathogenic variants in ULMS: c.236A>C and c.2446C>T. The c.236A>C variant has already been described in meningothelial meningioma and is associated with IL-6 signaling pathways and DNA damage response. The c.2446C>T mutation has been observed in large bowel adenocarcinoma and transitional cell carcinoma of the urinary system. Persistent *NOTCH2* signaling is largely associated with poor clinical prognosis. In addition, it increases resistance to chemotherapy and radiotherapy, making these cancers less sensitive to treatment (40). *HER2* mutations have emerged as therapeutic targets for a variety of tumors. Anti-HER2 therapies are effective against breast, lung, and cervical cancers (41).

In this study, we were able to identify several mutations that contribute to a better understanding of the biology of USs and UCSs. Even with the limitations associated with rare tumors, we identified genetic alterations that might act as potential target markers for precision medicine-based approaches upon validation in larger cohorts. To date, there is no precise preoperative diagnostic test for these tumors. Although rare, such tumors are very aggressive and associated with a poor prognosis. Thus, even with small cohorts, the molecular profiling of USs and UCSs is extremely important to identify the changes driving the development of these tumors and provide powerful tools for diagnostic and prognostic tests as well as adequate treatment alternatives. Our study is the first DNA-sequencing study to investigate all histological types of USs and UCSs together and is an insightful contribution for defining the mutational repertoire of these rare tumors.

CONCLUSIONS

Using a platform to profile mutations in a panel of 409 genes, we identified that *TP53*, *ATM*, *PIK3CA*, *APC*, *MTOR*, *DICER1*, *TRRAP*, *KMT2D*, *TSC2*, *PDE4DIP*, and *JAK3* are the most frequently mutated genes in USs and UCSs. Considering common mutations among the different tumor types being evaluated, the *TP53* (4 UCS/4 ULMS/3 ESS), *ATM* (2 ULMS/2 ESS/1 UCS), and *KMT2D* (1 UCS/1 ULMS/1 ESS) genes could be indicators of similarities in neoplastic progression. As specific signature genes, ESS exhibited mutations in the *PDE4DIP*, *IGTA10*, and *DST* genes. UCS showed mutations in the *ERBB4* gene, and ULMS demonstrated exclusive alterations in the *NOTCH2* and *HER2* genes. Mutations in the *KMT2A* gene were observed exclusively in ULM and ULMS samples, and therefore, are potentially involved in the malignant transformation process. According to the Cytoscape platform, many genes that were mutated in the ULMS and ESS samples exhibit functions associated with the cellular response to hypoxia and peptide hormone stimulus. In UCS and ADS, most altered genes exhibit functions associated with phosphatidylinositol kinase activity and glycerophospholipid metabolic process. More studies should be conducted with a larger number of samples and functional analyses. However, the current screening contributes to the characterization of the complex genetic profile of USs and UCSs.

ACKNOWLEDGMENTS

The research received financial support from Fundação de Amparo à Pesquisa do Estado de São Paulo – FAPESP (process numbers: 2016/03163-6 and 2019/01109-2).

AUTHOR CONTRIBUTIONS

Da Costa LT and Dos Anjos LG were responsible for study conceptualization, literature organization and paper elaboration. Kagohara LT collaborated in analyses of data, manuscripts and reviews. Torrezan GT and De Paula CAA contributed to the study execution. Baracat EC and Carraro DM provided intellectual support. Carvalho KC analyzed the literature, critically reviewed the manuscript, supervised the research and developed the original idea.

REFERENCES

1. Wen KC, Horng HC, Wang PH, Chen YJ, Yen MS, Ng HT, et al. Uterine sarcoma Part I-Uterine leiomyosarcoma: The Topic Advisory Group systematic review. *Taiwan J Obstet Gynecol*. 2016;55(4):463-71. <https://doi.org/10.1016/j.tjog.2016.04.033>
2. WHO Classification of Tumours Editorial Board. *Female Genital Tumours*. Lyon (France): International Agency for Research on Cancer; 2020. WHO classification of tumours series, 5th ed.; vol. 4.
3. Gonzalez Dos Anjos L, de Almeida BC, Gomes de Almeida T, Mourão Lavorato Rocha A, De Nardo Maffazioli G, Soares FA, et al. Could miRNA Signatures be Useful for Predicting Uterine Sarcoma and Carcinosarcoma Prognosis and Treatment? *Cancers (Basel)*. 2018;10(9):315. <https://doi.org/10.3390/cancers10090315>
4. Mbatani N, Olawaiye AB, Prat J. Uterine sarcomas. *Int J Gynaecol Obstet*. 2018;143 Suppl 2:51-8. <https://doi.org/10.1002/ijgo.12613>
5. Tuyaerts S, Amant F. Endometrial Stromal Sarcomas: A Revision of Their Potential as Targets for Immunotherapy. *Vaccines (Basel)*. 2018;6(3):56. <https://doi.org/10.3390/vaccines6030056>
6. Ma X, Wang J, Wang J, Ma CX, Gao X, Patriub V, et al. The JAZF1-SUZ12 fusion protein disrupts PRC2 complexes and impairs chromatin repression during human endometrial stromal tumorigenesis. *Oncotarget*. 2017;8(3):4062-78. <https://doi.org/10.18632/oncotarget.13270>
7. Hrzenjak A. JAZF1/SUZ12 gene fusion in endometrial stromal sarcomas. *Orphanet J Rare Dis*. 2016;11:15. <https://doi.org/10.1186/s13023-016-0400-8>
8. Han L, Liu YJ, Ricciotti RW, Mantilla JG. A novel MBTD1-PHF1 gene fusion in endometrial stromal sarcoma: A case report and literature review. *Genes Chromosomes Cancer*. 2020;59(7):428-32. <https://doi.org/10.1002/gcc.22845>
9. Micci F, Brunetti M, Dal Cin P, Nucci MR, Gorunova L, Heim S, et al. Fusion of the genes BRD8 and PHF1 in endometrial stromal sarcoma. *Genes Chromosomes Cancer*. 2017;56(12):841-5. <https://doi.org/10.1002/gcc.22485>
10. Dewaele B, Przybyl J, Quattrone A, Finalet Ferreiro J, Vanspauwen V, Geerdens E, et al. Identification of a novel, recurrent MBTD1-CXorf67 fusion in low-grade endometrial stromal sarcoma. *Int J Cancer*. 2014;134(5):1112-22. <https://doi.org/10.1002/ijc.28440>
11. Choi YJ, Jung SH, Kim MS, Baek IP, Rhee JK, Lee SH, et al. Genomic landscape of endometrial stromal sarcoma of uterus. *Oncotarget*. 2015;6(32):33319-28. <https://doi.org/10.18632/oncotarget.5384>
12. Amant F, Coosemans A, Debiec-Rychter M, Timmerman D, Vergote I. Clinical management of uterine sarcomas. *Lancet Oncol*. 2009;10(12):1188-98. [https://doi.org/10.1016/S1470-2045\(09\)70226-8](https://doi.org/10.1016/S1470-2045(09)70226-8)
13. Seddon BM, Davda R. Uterine sarcomas--recent progress and future challenges. *Eur J Radiol*. 2011;78(1):30-40. <https://doi.org/10.1016/j.ejrad.2010.12.057>
14. Kobayashi H, Uekuri C, Akasaka J, Ito F, Shigemitsu A, Koike N, et al. The biology of uterine sarcomas: A review and update. *Mol Clin Oncol*. 2013;1(4):599-60. <https://doi.org/10.3892/mco.2013.124>
15. Cancer Genome Atlas Research Network.; Cancer Genome Atlas Research Network. Comprehensive and Integrated Genomic Characterization of Adult Soft Tissue Sarcomas. *Cell*. 2017;171(4):950-65.e28. <https://doi.org/10.1016/j.cell.2017.10.014>
16. Tsuyoshi H, Yoshida Y. Molecular biomarkers for uterine leiomyosarcoma and endometrial stromal sarcoma. *Cancer Sci*. 2018;109(6):1743-52. <https://doi.org/10.1111/cas.13613>
17. Cherniack AD, Shen H, Walter V, Stewart C, Murray BA, Bowlby R, et al. Integrated Molecular Characterization of Uterine Carcinosarcoma. *Cancer Cell*. 2017;31(3):411-23. <https://doi.org/10.1016/j.ccell.2017.02.010>
18. Bean GR, Anderson J, Sangoi AR, Krings G, Garg K. DICER1 mutations are frequent in müllerian adenocarcinomas and are independent of rhabdomyosarcomatous differentiation. *Mod Pathol*. 2019;32(2):280-9. <https://doi.org/10.1038/s41379-018-0132-5>



19. Berra, CM, Torrezan GT, de Paula CA, Hsieh R, Lourenço SV, Carraro DM. Use of uracil-DNA glycosylase enzyme to reduce DNA-related artifacts from formalin-fixed and paraffin-embedded tissues in diagnostic routine. *Appl Cancer Res.* 2019;39:1-6. <https://doi.org/10.1186/s41241-019-0075-2>
20. Shannon P, Markiel A, Ozier O, Baliga NS, Wang JT, Ramage D, et al. Cytoscape: a software environment for integrated models of biomolecular interaction networks. *Genome Res.* 2003;13(11):2498-504. <https://doi.org/10.1101/gr.1239303>
21. Shabani Azim F, Hourri H, Ghalavand Z, Nikmanesh B. Next Generation Sequencing in Clinical Oncology: Applications, Challenges and Promises: A Review Article. *Iran J Public Health.* 2018;47(10):1453-7.
22. Bailey MH, Tokheim C, Porta-Pardo E, Sengupta S, Bertrand D, Weerasinghe A, et al. Comprehensive Characterization of Cancer Driver Genes and Mutations. *Cell.* 2018;174(4):1034-5. Erratum for: *Cell.* 2018;173(2):371-85.e18. <https://doi.org/10.1016/j.cell.2018.02.060>
23. Alqahtani A, Ayesh HSK, Halawani H. PIK3CA Gene Mutations in Solid Malignancies: Association with Clinicopathological Parameters and Prognosis. *Cancers (Basel).* 2019;12(1):93. <https://doi.org/10.3390/cancers12010093>
24. Samuels Y, Wang Z, Bardelli A, Silliman N, Ptak J, Szabo S, et al. High frequency of mutations of the PIK3CA gene in human cancers. *Science.* 2004;304(5670):554. <https://doi.org/10.1126/science.1096502>
25. Cuppens T, Annibali D, Coosemans A, Trovik J, Ter Haar N, Colas E, et al. Potential Targets' Analysis Reveals Dual PI3K/mTOR Pathway Inhibition as a Promising Therapeutic Strategy for Uterine Leiomyosarcomas-an ENITEC Group Initiative. *Clin Cancer Res.* 2017;23(5):1274-85. <https://doi.org/10.1158/1078-0432.CCR-16-2149>
26. Ueda R, Kohanbash G, Sasaki K, Fujita M, Zhu X, Kastenhuber ER, et al. Dicer-regulated microRNAs 222 and 339 promote resistance of cancer cells to cytotoxic T-lymphocytes by down-regulation of ICAM-1. *Proc Natl Acad Sci U S A.* 2009;106(26):10746-51. <https://doi.org/10.1073/pnas.0811817106>
27. de Almeida BC, Garcia N, Maffazioli G, dos Anjos LG, Baracat EC, Carvalho KC. Oncomirs Expression Profiling in Uterine Leiomyosarcoma Cells. *Int J Mol Sci.* 2017;19(1):52. <https://doi.org/10.3390/ijms19010052>
28. Teicher BA. Searching for molecular targets in sarcoma. *Biochem Pharmacol.* 2012;84(1):1-10. <https://doi.org/10.1016/j.bcp.2012.02.009>
29. Roy M, Kumar S, Bhatla N, Ray MD, Kumar L, Jain D, et al. Androgen Receptor Expression in Endometrial Stromal Sarcoma: Correlation With Clinicopathologic Features. *Int J Gynecol Pathol.* 2017;36(5):420-7. <https://doi.org/10.1097/PGP.0000000000000353>
30. Baek MH, Park JY, Park Y, Kim KR, Kim DY, Suh DS, et al. Androgen receptor as a prognostic biomarker and therapeutic target in uterine leiomyosarcoma. *J Gynecol Oncol.* 2018;29(3):e30. <https://doi.org/10.3802/jgo.2018.29.e30>
31. Yamaguchi M, Kusunoki S, Hirayama T, Fujino K, Terao Y, Itakura A. Case of leiomyosarcoma arising from subserosal leiomyoma. *J Obstet Gynaecol Res.* 2019;45(9):1944-7. <https://doi.org/10.1111/jog.14037>
32. dos Anjos LG, da Cunha IW, Baracat EC, Carvalho KC. Genetic and Epigenetic Features in Uterine Smooth Muscle Tumors: An Update. *Clin Oncol.* 2019;4(1):1637.
33. National Center for Biotechnology Information. ClinVar; [VCV000430818.2], Available from: <https://www.ncbi.nlm.nih.gov/clinvar/variation/VCV000430818.2> [accessed Apr 21, 2020].
34. Sobreira N, Brucato M, Zhang L, Ladd-Acosta C, Ongaco C, Romm J, et al. Patients with a Kabuki syndrome phenotype demonstrate DNA methylation abnormalities. *Eur J Hum Genet.* 2017;25(12):1335-44. <https://doi.org/10.1038/s41431-017-0023-0>
35. Tate JG, Bamford S, Jubb HC, Sondka Z, Beare DM, Bindal N, et al. COSMIC: the Catalogue Of Somatic Mutations In Cancer. *Nucleic Acids Res.* 2019;47(D1):D941-7. <https://doi.org/10.1093/nar/gky1015>
36. Er TK, Su YF, Wu CC, Chen CC, Wang J, Hsieh TH, et al. Targeted next-generation sequencing for molecular diagnosis of endometriosis-associated ovarian cancer. *J Mol Med.* 2016;94(7):835-47. <https://doi.org/10.1007/s00109-016-1395-2>
37. Soung YH, Lee JW, Kim SY, Wang YP, Jo KH, Moon SW, et al. Somatic mutations of the ERBB4 kinase domain in human cancers. *Int J Cancer.* 2006;118(6):1426-9. <https://doi.org/10.1002/ijc.21507>
38. Hollmén M, Elenius K. Potential of ErbB4 antibodies for cancer therapy. *Future Oncol.* 2010;6(1):37-53. <https://doi.org/10.2217/fon.09.144>
39. Buerki RA, Horbinski CM, Kruser T, Horowitz PM, James CD, Lukas RV. An overview of meningiomas. *Future Oncol.* 2018;14(21):2161-77. <https://doi.org/10.2217/fon-2018-0006>
40. Xiu MX, Liu YM. The role of oncogenic Notch2 signaling in cancer: a novel therapeutic target. *Am J Cancer Res.* 2019;9(5):837-54.
41. Cocco E, Lopez S, Santin AD, Scaltriti M. Prevalence and role of HER2 mutations in cancer. *Pharmacol Ther.* 2019;199:188-96. <https://doi.org/10.1016/j.pharmthera.2019.03.010>



Table S1 - Ion AmpliSeq Comprehensive Cancer Panel target gene list.

1	ABL1	GBL	EP300	GATA2	LAMP1	MYD88	PKHD1	SMARCA4	WHSC1
2	ABL2	CCND1	EP400	GATA3	LCK	MYH11	PLAG1	SMARCB1	WRN
3	ACVR2A	CCND2	EPHA3	GDNF	LIFR	MYH9	PLCG1	SMO	WT1
4	ADAMTS20	CCNE1	EPHA7	GNAI1	LPHN3	NBN	PLEKHG5	SMUG1	XPA
5	AFF1	CD79A	EPH1	GNAQ	POT1	NCOA1	PML	SOC51	XPC
6	AFF3	CD79B	EPH4	GNAS	LPP	NCOA2	PMS1	SOX11	XPO1
7	AKAP9	CDC73	EPH6	GPR124	LRP1B	NCOA4	PMS2	SOX2	XRCC2
8	AKT1	CDH1	ERBB2	GRM8	LTF	NF1	POU5F1	SRC	ZNF384
9	AKT2	CDH11	ERBB3	GUCY1A2	LTK	NF2	PPARG	SSX1	ZNF521
10	AKT3	CDH2	ERBB4	HCAR1	MAF	NFE2L2	PPP2R1A	STK11	
11	ALK	CDH20	ERCC1	HIF1A	MAFB	NFKB1	PRDM1	STK36	
12	APC	CDH5	ERCC2	HLF	MAGEA1	NFKB2	PRKAR1A	SUFU	
13	AR	CDK12	ERCC3	HNF1A	MAGI1	NIN	PRKDC	SYK	
14	ARID1A	CDK4	ERCC4	HOOK3	MALTI	NKX2-1	PSIP1	SYNE1	
15	ARID2	CDK6	ERCC5	HRAS	MAML2	NLRP1	PTCH1	TAF1	
16	ARNT	CDK8	ERG	HSP90AA1	MAP2K1	NOTCH1	PTEN	TAF1L	
17	ASXL1	CDKN2A	ESR1	HSP90AB1	MAP2K2	NOTCH2	PTGS2	TAL1	
18	ATF1	CDKN2B	ETS1	ICK	MAP2K4	NOTCH4	PTPN11	TBX22	
19	ATM	CDKN2C	ETV1	IDH1	MAP3K7	NPM1	PTPRD	TCF12	
20	ATR	CEBPA	ETV4	IDH2	MAPK1	NRAS	PTPRT	TCF3	
21	ATRX	CHEK1	EXT1	IGFIR	MAPK8	NSD1	RAD50	TCF7L1	
22	AURKA	CHEK2	EXT2	IGF2	MARK1	NTRK1	RAF1	TCF7L2	
23	AURKB	CIC	EZH2	IGF2R	MARK4	NTRK3	RALGDS	TCL1A	
24	AURKC	CKS1B	FAM123B	IKBK1	MBD1	NUMA1	RARA	TET1	
25	AXL	CMPK1	FANCA	IKBKE	MCL1	NUP214	RB1	TET2	
26	BAB3	COL1A1	FANCC	IKZF1	MDM2	NUP98	RECQL4	TFE3	
27	BAP1	CRBN	FANCD2	IL2	MDM4	PAK3	REL	TGFBR2	
28	BCL10	CREB1	FANCF	IL21R	MEN1	PALB2	RET	TGM7	
29	BCL11A	CREBBP	FANCG	IL6ST	MET	PARP1	RHOH	THBS1	
30	BCL11B	CRKL	FAS	IL7R	MITF	PAX3	RNASEL	TIMP3	
31	BCL2	CRTC1	FBXW7	ING4	MLH1	PAX5	RNF2	TLR4	
32	BCL2L1	CSF1R	FGFR1	IRF4	MLL	PAX7	RNF213	TLX1	
33	BCL2L2	CSMD3	FGFR2	IRS2	MLL2	PAX8	ROSI	TNFAIP3	
34	BCL3	CTNNA1	FGFR3	ITGA10	MLL3	PBRM1	RPS6KA2	TNFRSF14	
35	BCL6	CTNNA1	FGFR4	ITGA9	MLLT10	PBX1	RRM1	TNK2	
36	BCL9	CTNNA1	FH	ITGB2	MMP2	PDE4DIP	RUNX1	TOP1	
37	BCR	CYP2C19	FLCN	ITGB3	MN1	PDGFB	RUNX1T1	TP53	
38	BIRC2	CYP2D6	FLI1	JAK1	MPL	PDGFRA	SAMD9	TPR	
39	BIRC5	DAXX	FLT1	JAK2	MRE11A	PDGFRB	SBDS	TRIM24	
40	BLM	DCC	FLT3	JAK3	MSH2	PER1	SDHA	TRIM33	
41	BLM	DBB2	FLT4	JUN	MSH6	PGAP3	SDHB	TRIP11	
42	BLNK	DDIT3	FN1	KAT6A	MTOR	PHOX2B	SDHC	TRRAP	
43	BMPR1A	DDR2	FOXL2	KAT6B	MTR	PIK3C2B	SDHD	TSC1	
44	BRAF	DEK	FOXO1	KDM5C	MTRR	PIK3CA	SEPT9	TSC2	
45	BRD3	DICER1	FOXO3	KDM6A	MUC1	PIK3CB	SETD2	TSHR	
46	BRIP1	DNMT3A	FOXP1	KDR	MUTYH	PIK3CD	SF3B1	UBR5	
47	BTK	DPYD	FOXP4	KEAP1	MYB	PIK3CG	SGK1	UGT1A1	
48	BUB1B	DST	FZRI	KIT	MYC	PIK3R1	SH2D1A	USP9X	
49	CARD11	EGFR	G6PD	KLIF6	MYCL1	PIK3R2	SMAD2	VHL	
50	CASC5	EML4	GATA1	KRAS	MYCN	PIK3R2	SMAD4	WAS	



Table S2 - Description of 153 potential somatic variants selected in 23 samples of uterine tumors.

Sample	Chr.Pos	Gene	HGVS c.	HGVS p.	Effect	
UCS2	3:178921549	<i>PIK3CA</i>	c.1031T>C	p.Val344Ala	Missense	
	6:94120318	<i>EPHA7</i>	c.733G>A	p.Ala245Thr	Missense	
	7:116339356	<i>MET</i>	c.218T>A	p.Leu73Ter	LOF: stop - gained	
	8:48776121	<i>PRKDC</i>	c.5586delT	p.Phe1862Leufs	LOF: frameshift	
	15:99500303	<i>IGF1R</i>	c.3736C>T	p.Arg1246Cys	Missense	
	17:7577547	<i>TP53</i>	c.734G>T	p.Gly245Val	Missense	
	22:33253291	<i>TIMP3</i>	c.260delC	p.Glu88Argfs	LOF: frameshift	
	UCS5	1:11227575	<i>MTOR</i>	c.4254-1G>A	r.spl?	LOF: splice - acceptor
		1:27105553	<i>ARID1A</i>	c.5164C>T	p.Arg1722Ter	LOF: stop - gained
		1:65310574	<i>JAK1</i>	c.2116-2A>G	r.spl?	LOF: splice - acceptor
3:178952085		<i>PIK3CA</i>	c.3140A>G	p.His1047Arg	Missense	
10:76735809		<i>KAT6B</i>	c.1714C>T	p.Arg572Cys	Missense	
10:97969609		<i>BLNK</i>	c.731C>T	p.Pro244Leu	Missense	
11:108114777		<i>ATM</i>	c.594C>A	p.Cys198Ter	LOF: stop - gained	
14:95572101		<i>DICER1</i>	c.3007C>T	p.Arg1003Ter	LOF: stop - gained	
17:29588751		<i>NF1</i>	c.4600C>T	p.Arg1534Ter	LOF: stop - gained	
17:29665110		<i>NF1</i>	c.6772C>T	p.Arg2258Ter	LOF: stop - gained	
19:45260400		<i>BCL3</i>	c.646C>T	p.Arg216Cys	Missense	
1:47685756		<i>TAL1</i>	c.632G>A	p.Arg211His	Missense	
2:25469168		<i>DNMT3A</i>	c.1290T>G	p.Asn430Lys	Missense	
2:212587219		<i>ERBB4</i>	c.782A>C	p.Gln261Pro	Missense	
7:98513427		<i>TRRAP</i>	c.2281T>C	p.Arg761Trp	Missense	
9:37015073		<i>PAX5</i>	c.331G>A	p.Ala111Thr	Missense	
19:11098401		<i>SMARCA4</i>	c.919C>T	p.Pro307Ser	Missense	
20:36030940		<i>SRC</i>	c.1219G>A	p.Asp407Asn	Missense	
X:44942716		<i>KDM6A</i>	c.3452A>G	p.Gln1151Arg	Missense	
X:66766207		<i>AR</i>	c.1219C>T	p.Arg407Cys	Missense	
UCS9	9:139391355	<i>NOTCH1</i>	c.6836C>T	p.Ala2279Val	Missense	
	10:123298226	<i>FGFR2</i>	c.628C>T	p.Arg210Ter	LOF: stop - gained	
	12:49444719	<i>KMT2D</i>	c.2747C>T	p.Pro916Leu	Missense	
	15:40916649	<i>KNL1</i>	c.4265G>A	p.Arg1422Gln	Missense	
	17:7578442	<i>TP53</i>	c.488A>G	p.Tyr163Cys	Missense	
	3:52440867	<i>BAP1</i>	c.637C>T	p.Arg213Cys	Missense	
	21:39755729	<i>ERG</i>	c.1057G>A	p.Glu353Lys	Missense	
UCS13	3:178916854	<i>PIK3CA</i>	c.241G>A	p.Glu81Lys	Missense	
	11:71726283	<i>NUMA1</i>	c.2266G>T	p.Glu756Ter	LOF: stop - gained	
	13:29001422	<i>FLT1</i>	c.1310C>T	p.Ser437Leu	Missense	
	14:95574253	<i>DICER1</i>	c.2614G>A	p.Ala872Thr	Missense	
	17:7577534	<i>TP53</i>	c.747G>T	p.Arg249Ser	Missense	
	5:176636902	<i>NSD1</i>	c.1502A>G	p.Lys501Arg	Missense	
	7:98609947	<i>TRRAP</i>	c.11549G>A	p.Arg3850His	Missense	
UCS19	2:212295800	<i>ERBB4</i>	c.2513G>A	p.Arg838Gln	Missense	
	9:5126715	<i>JAK2</i>	c.3323A>G	p.Asn1108Ser	Missense	
	17:7577580	<i>TP53</i>	c.701A>G	p.Tyr234Cys	Missense	
	17:37829120	<i>PGAP3</i>	c.900-1G>A	r.spl?	LOF: splice - acceptor	
ULMS38	1:120458122	<i>NOTCH2</i>	c.7223T>A	p.Leu2408His	Missense	
	6:51914991	<i>PKHD1</i>	c.2243C>T	p.Ala748Val	Missense	
	16:23646942	<i>PALB2</i>	c.925A>G	p.Ile309Val	Missense	
	17:5462805	<i>NLRP1</i>	c.1211G>A	p.Arg404Gln	Missense	
	17:37864584	<i>ERBB2</i>	c.236A>C	p.Glu79Ala	Missense	
	3:65425588	<i>MAG11</i>	c.1234_1236delCAG	p.Gln421del	Inframe - deletion	
ULMS39	19:17937659	<i>JAK3</i>	c.3268G>A	p.Ala1090Thr	Missense	
	3:188327501	<i>LPP</i>	c.982C>T	p.Arg328Trp	Missense	
	7:142562071	<i>EPHB6</i>	c.513_515delCTC	p.Ser176del	LOF: disruptive - inframe - del	
ULMS40	17:7577545	<i>TP53</i>	c.736A>G	p.Met246Val	Missense	
ULMS40	2:100218031	<i>AFF3</i>	c.1310_1312delGCA	p.Ser444del	LOF: disruptive - inframe - del	
ULMS40	11:108139268	<i>ATM</i>	c.2770C>T	p.Arg924Trp	Missense	
	17:7577120	<i>TP53</i>	c.818G>A	p.Arg273His	Missense	
	17:37881117	<i>ERBB2</i>	c.2446C>T	p.Arg816Cys	Missense	
	X:76891445	<i>ATRX</i>	c.4660A>T	p.Arg1554Ter	LOF: stop - gained	
ULMS45	3:128204775	<i>GATA2</i>	c.666G>C	p.Lys222Asn	Missense	
	11:108160506	<i>ATM</i>	c.4414T>G	p.Leu1472Val	Missense	
	12:121437187	<i>HNF1A</i>	c.1618A>G	p.Lys540Glu	Missense	
	17:7578290	<i>TP53</i>	c.560-1G>C	r.spl?	LOF: splice - acceptor	
	16:2135281	<i>TSC2</i>	c.4620C>A	p.Tyr1540Ter	LOF: stop - gained	
ULMS50b	2:29432740	<i>ALK</i>	c.3748A>G	p.Ile1250Val	Missense	
ULMS52	1:6528318	<i>PLEKHG5</i>	c.2815C>T	p.Arg939Cys	Missense	
	1:120459251	<i>NOTCH2</i>	c.6094C>A	p.His2032Asn	Missense	
	9:139400980	<i>NOTCH1</i>	c.4013C>T	p.Ala1338Val	Missense	
	11:118377142	<i>KMT2A</i>	c.10535C>T	p.Pro3512Leu	Missense	



Table S2 - Continued.

Sample	Chr:Pos	Gene	HGVS c.	HGVS p.	Effect
ULMS59	12:49416396	<i>KMT2D</i>	c.16315C>T	p.Arg5439Trp	Missense
	13:26978093	<i>CDK8</i>	c.1270C>T	p.Arg424Cys	Missense
	16:2130319	<i>TSC2</i>	c.3551C>T	p.Ala1184Val	Missense
	16:3779521	<i>CREBBP</i>	c.5527T>C	p.Cys1843Arg	Missense
	16:3790470	<i>CREBBP</i>	c.4063G>A	p.Gly1355Arg	Missense
	17:7574017	<i>TP53</i>	c.1010G>A	p.Arg337His	Missense
	22:36678790	<i>MYH9</i>	c.5807G>A	p.Arg1936Gln	Missense
	5:112173857	<i>APC</i>	c.2566C>T	p.Arg856Cys	Missense
	6:135511289	<i>MYB</i>	c.331G>A	p.Gly111Ser	Missense
	6:135539101	<i>MYB</i>	c.2269C>T	p.Arg757Trp	Missense
	6:152832196	<i>SYNE1</i>	c.352C>T	p.Arg118Ter	LOF: stop - gained
	7:2946463	<i>CARD11</i>	c.3274C>T	p.Arg1092Ter	LOF: stop - gained
	18:22806393	<i>ZNF521</i>	c.1489C>T	p.Arg497Ter	LOF: stop - gained
	18:47803035	<i>MBD1</i>	c.472C>T	p.Arg158Ter	LOF: stop - gained
ESS2 (LG-ESS)	20:57429026	<i>GNAS</i>	c.706G>A	p.Asp236Asn	Missense
	20:57480457	<i>GNAS</i>	c.2381A>C	p.Lys794Thr	Missense
	22:30069262	<i>NF2</i>	c.1127G>A	p.Arg376Gln	Missense
	6:152706896	<i>SYNE1</i>	c.8565G>A	p.Trp2855Ter	LOF: stop - gained
	11:108175463	<i>ATM</i>	c.5558A>T	p.Asp1853Val	Missense
	14:81610269	<i>TSHR</i>	c.1867G>T	p.Ala623Ser	Missense
	17:7577121	<i>TP53</i>	c.817C>T	p.Arg273Cys	Missense
	17:7577139	<i>TP53</i>	c.799C>T	p.Arg267Trp	Missense
	19:3119273	<i>GNA11</i>	c.805G>A	p.Val269Ile	Missense
	22:41553308	<i>EP300</i>	c.3397C>T	p.Arg1133Trp	Missense
ESS3	1:145015874	<i>PDE4DIP</i>	c.214C>T	p.Arg72Ter	LOF: stop - gained
	5:112154777	<i>APC</i>	c.1048T>C	p.Ser350Pro	Missense
	5:112162855	<i>APC</i>	c.1459G>A	p.Gly487Arg	Missense
	6:56328464	<i>DST</i>	c.16429C>T	p.Arg5477Trp	Missense
	12:49418436	<i>KMT2D</i>	c.15977T>C	p.Leu5326Pro	Missense
	17:7578176	<i>TP53</i>	c.672 + 1G>A	r.spl?	LOF: splice - donor
	17:29556250	<i>NF1</i>	c.2617C>T	p.Arg873Cys	Missense
ESS4	17:29677234	<i>NF1</i>	c.7355G>T	p.Arg2452Leu	Missense
	11:108141990	<i>ATM</i>	c.2934delT	p.Leu979Cysfs	LOF: frameshift
	16:3820773	<i>CREBBP</i>	c.2678C>T	p.Ser893Leu	Missense
ESS5	1:11217330	<i>MTOR</i>	c.4348T>G	p.Tyr1450Asp	Missense
	14:51227050	<i>NIN</i>	c.1924G>A	p.Glu642Lys	Missense
ESS7	19:17937659	<i>JAK3</i>	c.3268G>A	p.Ala1090Thr	Missense
	20:41101170	<i>PTPRT</i>	c.1186G>A	p.Val396Ile	Missense
	6:33287248	<i>DAXX</i>	c.1885G>A	p.Val629Ile	Missense
	6:117710646	<i>ROS1</i>	c.1626delT	p.Phe542Leufs	LOF: frameshift
ESS7	14:95590677	<i>DICER1</i>	c.1232C>A	p.Ser411Ter	LOF: stop - gained
	X:76939115	<i>ATRX</i>	c.1633C>G	p.Gln545Glu	Missense
ESS9	1:144906139	<i>PDE4DIP</i>	c.2494delC	p.Gln832Argfs	LOF: frameshift
	1:145536012	<i>ITGA10</i>	c.2104G>A	p.Ala702Thr	Missense
	3:178936091	<i>PIK3CA</i>	c.1633G>A	p.Glu545Lys	Missense
	4:55564641	<i>KIT</i>	c.529C>T	p.Arg177Cys	Missense
	4:55976709	<i>KDR</i>	c.1116G>C	p.Glu372Asp	Missense
	5:112175711	<i>APC</i>	c.4420G>A	p.Ala1474Thr	Missense
	5:180048651	<i>FLT4</i>	c.1911C>G	p.Ser637Arg	Missense
	1:145015874	<i>PDE4DIP</i>	c.214C>T	p.Arg72Ter	LOF: stop - gained
	1:145536012	<i>ITGA10</i>	c.2104G>A	p.Ala702Thr	Missense
	2:142567932	<i>LRP1B</i>	c.121G>A	p.Asp41Asn	Missense
	4:153332477	<i>FBXW7</i>	c.479C>T	p.Pro160Leu	Missense
	6:56328464	<i>DST</i>	c.16429C>T	p.Arg5477Trp	Missense
	6:135516944	<i>MYB</i>	c.1007C>T	p.Thr336Ile	Missense
	7:91570414	<i>AKAP9</i>	c.1A>G	p.Met1?	LOF: initiator - codon
	17:7578176	<i>TP53</i>	c.672 + 1G>A	r.spl?	LOF: splice - donor
	X:41056743	<i>USP9X</i>	c.4360delG	p.Gly1454Glufs	LOF: frameshift
ADS2	X:66863156	<i>AR</i>	c.1675A>T	p.Thr559Ser	Missense
	1:162748436	<i>DDR2</i>	c.2350T>C	p.Cys784Arg	Missense
	2:25467477	<i>DNMT3A</i>	c.1599C>A	p.Tyr533Ter	LOF: stop - gained
	2:209110123	<i>IDH1</i>	c.440C>A	p.Pro147His	Missense
	3:38182306	<i>MYD88</i>	c.766T>C	p.Phe256Leu	Missense
	5:131927073	<i>RAD50</i>	c.1610delA	p.Met538Trpfs	LOF: frameshift
	6:33288629	<i>DAXX</i>	c.959A>G	p.Gln320Arg	Missense
	6:93979315	<i>EPHA7</i>	c.1513C>A	p.Leu505Met	Missense
	7:98501128	<i>TRRAP</i>	c.1024G>T	p.Glu342Ter	LOF: stop - gained
	8:48711786	<i>PRKDC</i>	c.10279G>T	p.Glu3427Ter	LOF: stop - gained
9:98209391	<i>PTCH1</i>	c.4147C>A	p.Pro1383Thr	Missense	



Table S2 - Continued.

Sample	Chr:Pos	Gene	HGVS c.	HGVS p.	Effect
	10:76781925	<i>KAT6B</i>	c.3308_3310delAAG	p.Glu1104del	LOF: disruptive – inframe - del
	11:106558436	<i>GUCY1A2</i>	c.2131G>T	p.Glu711Ter	LOF: stop - gained
	15:90630454	<i>IDH2</i>	c.857A>G	p.Glu286Gly	Missense
	16:2138078	<i>TSC2</i>	c.5098G>T	p.Ala1700Ser	Missense
	22:29121048	<i>CHEK2</i>	c.638T>C	p.Val213Ala	Missense
	X:53223847	<i>KDM5C</i>	c.3512A>G	p.Lys1171Arg	Missense
ULM119	7:116403114	<i>MET</i>	c.2429A>C	p.His810Pro	Missense
	22:39621795	<i>PDGFB</i>	c.659dupA	p.Lys222Glnfs	LOF: frameshift
ULM143	1:11307996	<i>MTOR</i>	c.995_996dupGG	p.Leu333Glyfs	LOF: frameshift
	9:32634260	<i>TAF1L</i>	c.1318A>G	p.Ile440Val	Missense
	19:17945696	<i>JAK3</i>	c.2164G>A	p.Val722Ile	Missense
ULM152	8:41791030	<i>KAT6A</i>	c.4708G>A	p.Asp1570Asn	Missense
	11:118344893	<i>KMT2A</i>	c.3019G>T	p.Gly1007Cys	Missense
	19:1207176	<i>STK11</i>	c.263_264insC	p.Asn90Glnfs	LOF: frameshift